2026

IMMC Summary Sheet

Team Control Number:**IMMC26402965**

Problem Chosen:**B**

Summary

Background and Objectives

Solar energy is developing rapidly as a clean energy source, but there is a trade-off between power generation efficiency and cost for different installation methods. Our primary object is to build a mathematical model that comprehensively considers power generation efficiency and economic costs, evaluate the cost-effectiveness of three installation methods, and extend the model to different regions.

Modeling Approach

Our power generation model integrates the Kasten-Young air mass model, the Sandia Array Performance Model, and the PVWatts model, considering factors such as solar position, angle of incidence, irradiance, and temperature to calculate the actual power output of different installation methods.

The economic model introduces capital expenditure and annual operational expenditure, using the Levelized Cost of Energy as the core evaluation metric to reflect the unit cost of electricity generation over the system's entire lifecycle.

Application and Validation

We select three cities—Chongqing, Urumqi, and Lhasa—as case studies, and results show that in sun-rich Lhasa and Urumqi, the dual-axis tracking system significantly outperforms the others in power generation, with the lowest or similar LCOE compared to the fixed-tilt system. In contrast, in Chongqing, which has weaker sunlight, the fixed-tilt system is more economical.

By adjusting cost parameters, the model can be adapted to other countries (e.g., the U.S.), demonstrating good generalizability.

A "manually adjusted mount" option is proposed and analyzed economically, showing limited impact in sun-rich areas but potential cost benefits in areas with weaker sunlight.

Conclusions and Recommendations

Tracking systems significantly improve power generation efficiency and are economically advantageous in regions with abundant sunlight, dual-axis system performing particularly well.

In regions with weaker sunlight, fixed panels are more competitive due to their lower costs and simpler maintenance.

Keywords: Photovoltaic system, cost-effectiveness.

Contents

1 Introduction

1.1 Background

Solar energy is widely regarded as a promising and environmentally friendly source of electricity. Photovoltaic technology, in particular, accounted for 456 GW of electricity generation in 2023, reducing 0.92 gigatons of carbon dioxide emissions [1]. Photovoltaic application is observed to surge in 2024, producing electricity between 553 and 601 GW, with the endeavors of China, the US, and the Europe [2]. While similar advances in photovoltaic application are ubiquitous in many parts of the world, it remains unclear which way of installation of photovoltaic panels is the most cost-effective.

In specific, there are three types of installation: 1) fixed position with dwindled power output due to light-incidence-related cosine effect, reflective effects, and loss of photovoltaic efficiency; 2) single-axis configuration that rotates panels to compensate for the effects of light incidence yet still affected by seasonal changes of the sun's position; and 3) dual-axis configuration that perfectly guarantees zero incidence by rotating the panels around two axes but has higher costs of complex installation and maintenance.

Overall, the benefits and drawbacks of each installation are so intricate that it is hard to determine the best configuration that can be applied under specific circumstances. This paper aims to fill the research gap by systematically modeling the cost-effectiveness of each solar panel installation, pinpointing the boundaries between distinct conditions which lead to a shift in the choice of installation.

1.2 Problem Restatement

Task 1: The primary objective is to construct a mathematical model that estimates and compares the cost-effectiveness of three solar panel installation strategies, considering factors such as geographic location and use of installation (private or industrial).

Task 2: To ensure that the model is generalizable, we must account for the prices and technology outside China and expand our model.

Task 3: This question affords one more option of installation; that is the "manually adjusted mount" that alters the panel's position with a period of half a year.

Task 4: In this task, we must evaluate based on our model the applicability of the tracking system.

1.3 Assumptions And Justifications

Assumption 1: The sunlight intensity in four seasons retains the same. Although, in fact, the earth has an oval orbit around the sun, the differences between light intensities in different seasons are barely quantifiable. Therefore, we consider sunlight intensity as a constant.

Assumption 2: During a particular season, the trajectory of the sun does not change. This assumption avoids the case in which the consideration of the subtle daily change in the sun's position overly complicates our model.

Assumption 3: We assume to neglect the influence of weather, such as overcast or snow that block the sunlight. Since the weather is barely predictable, we have to abandon this influential factor.

2 Problem 1

2.1 Power Output

Mentioned symbols in this subsection and their meanings are listed in Table 1.

To model the cost-effectiveness of the three installation strategies, we first have to understand the factors of photovoltaic electricity production. One such factor is the air mass: the farther light travels in the atmosphere, the more energy will be diffused. According to Kasten-Young Model, the equation of air mass is [3]:

$$AM = \frac{1}{cos(\theta_z) + 0.50572 \cdot (96.07995 - \theta_z)^{-1.6364}} \tag{1}$$

The consideration of air mass is essential for calculating the effective irradiance. Moreover, more factors should be involved, such as the angle of incidence. Using the solar zenith and solar azimuth, we are able to primarily calculate the unit vector of the sunlight, which determines the angle of incidence ($\vec{n}$ represents the normal vector):

$$\begin{cases} \vec{s} = \begin{bmatrix} sin(\theta_z) \cdot sin(\theta_a) \\ sin(\theta_z) \cdot cos(\theta_a) \\ cos(\theta_z) \end{bmatrix} \\ \\ cos(AOI) = \vec{s} \cdot \vec{n} \end{cases} \tag{2}$$

The incidence angle can be then included in quantifying beam radiance and diffusion radiance from the ground, which are evident differences between installation strategies. Comparing fixed configuration with single-axis configuration, for example, the latter is expected to have greater beam radiance due to the ability to rotate according to the sun's position for the sake of minimum reflection. The Sandia Array Performance Model satisfies all these considerations, and its equation is the following [4]:

$$E_e = f_1(AM) \cdot (E_b \cdot cos(AOI) \cdot f_2(AOI) + f_d \cdot E_d \tag{3}$$

Here, f_d is a constant representing the proportion of unreflected diffusion irradiance; $f_1(AM)$ and $f_2(AOI)$ are polynomial correction functions of AM and AOI,

Table 1 Symbols and Explanation

Symbol	Unit	Explanation
θ_z	radian	The solar zenith: measure of the angle determined by vertical direction and the direction of sunlight.
θ_a	radian	The solar azimuth: measure of the angle determined by north direction and the direction of sunlight.
$\vec{s}$	/	The unit vector of the sun's rays.
AM	/	Airmass: the relative distance of light traveling through the atmosphere ($\frac{\text{actual distance}}{\text{distance at } \theta_z = 0}$).
AOI	radian	The angle of incidence.
P_{dc}	W	The actual power generated by photovoltaic cells.
P_0	W	The power under standard test condition.
E_e	W/m^2	The actual effective irradiance.
E_b	W/m^2	The beam (direct light) irradiance.
E_d	W/m^2	The irradiance of diffusion.
E_0	W/m^2	The effective irradiance under standard test condition (fixedly $1000W/m^2$).
T_{cell}	$°C$	The actual temperature of photovoltaic cells.
T_A	$°C$	The environment temperature.
ΔT	$°C$	The difference between the temperature of non-working photovoltaic cells and that of environment ($30°C$ by default).
T_{ref}	$°C$	The reference temperature of photovoltaic cells (normally $25°C$).
γ	$°C^{-1}$	Temperature constant (normally $-0.004°C^{-1}$).
U_{dc}	V	The actual voltage of direct current.
$U_{dc,rt}$	V	The rating (maximum) voltage of direct current.
η_v	/	The voltage derating index.
$P_{dc,eff}$	W	The actual effective power of direct current.
$P_{dc,rt}$	W	The rating power of direct current.
P_{act}	W	The power of direct current needed to activate inverter.
P_{ac}	W	The actual power output of alternating current.
P_{ac0}	W	The rating power output of alternating current.

respectively, whose constants can be determined by fitting.

$$\begin{cases} f_1(AM) = a_0 + a_1 \cdot AM + a_2 \cdot AM^2 + a_3 \cdot AM^3 + a_4 \cdot AM^4 \\ f_2(AOI) = b_0 + b_1 \cdot AOI + b_2 \cdot AOI^2 + b_3 \cdot AOI^3 + b_4 \cdot AOI^4 + b_5 \cdot AOI^5 \end{cases} \tag{4}$$

Next, we can apply the equation in the PVWatts Model to compute the actual power production of each strategy of installation [5]. This model is universally applied in determining direct current power, with additive regard to the influence of cell temperature:

$$\begin{cases} T_{cell} = T_A + \frac{E_e}{E_0} \cdot \Delta T \\ P_{dc} = P_0 \cdot \frac{E_e}{E_0} \cdot [1 + \gamma \cdot (T_{cell} - T_{ref})] \end{cases} \tag{5}$$

Eventually, direct current should be transformed into alternating current. The Sandia Inverter Model suffices illustrating the converting process of direct current to alternating current [6]. The first step in this model is to normalize the voltage of direct current, the result nominated as v_{norm}:

$$v_{norm} = \frac{U_{dc}}{U_{dc,rt}} \tag{6}$$

This normalized value is used to fit a quadratic polynomial that calculates the index of voltage derating that represents the effective proportion of the power output of direct current.

$$\eta_v = a + b \cdot v_{norm} + c \cdot v_{norm}^2 \tag{7}$$

Here, constants a, b, c are determined by fitting, and then the effective power of direct current is:

$$P_{dc,eff} = P_{dc} \cdot \eta_v \tag{8}$$

Afterward, the current will be inverted to the alternating form. If the effective power of direct current is lower than the activation power of the inverter, there will be no alternating current output because of non-working inverter. If $P_{dc,eff}$ is higher than the activation power but lower than the rating power of inverters, the ratio of actual power output of alternating current to the rating power output equals that of effective power of direct current to its rating power. If $P_{dc,eff}$ is greater than $P_{dc,rt}$, the surplus will be cut and the alternating current output is the rating power. These are shown in the following equation:

$$P_{ac} = \begin{cases} 0, & P_{dc,eff} < P_{act} \\ P_{ac0} \cdot \left(\frac{P_{dc,eff}}{P_{dc,rt}} \right), & P_{dc,eff} \le P_{dc,rt} \\ P_{ac0}, & P_{dc,eff} > P_{dc,rt} \end{cases} \tag{9}$$

2.2 Economic Effects

Mentioned symbols in this subsection and their meanings are listed in Table 2.

To quantify the economic performance of fixed-tilt, single-axis, and dual-axis photovoltaic systems, we develop a cost model that incorporates both upfront investment and long-term operational expenses. The levelized cost of energy (LCOE) is then used as the unified evaluation metric, as it reflects the average unit cost of electricity generation over the entire lifetime of the system. A lower LCOE indicates that the system produces electricity more economically, and thus determines whether solar trackers function as a practical enhancement or merely a costly "toy."

The first component of the economic model is the capital expenditure (CAPEX), which represents all one-time construction and installation expenses. Since photovoltaic modules, inverters, balance-of-system components, supporting racks, and trackers are all scaled with the installed system capacity, their costs are aggregated on a per-kilowatt basis and multiplied by the rated capacity. Additional expenditures arising from permitting, engineering, construction, and site preparation are incorporated through a multiplicative factor, resulting in the following expression for total upfront investment:

$$\mathrm{CAPEX} = P_{\mathrm{rated}} \cdot (C_{\mathrm{mod}} + C_{\mathrm{inv}} + C_{\mathrm{bos}} + C_{\mathrm{rack}} + C_{\mathrm{tracker}}) \cdot (1 + C_{\mathrm{perm}})$$

The parameters recorded in Figure 1 specify these cost terms under the static, single-axis, and dual-axis scenarios. Notably, C_{tracker} is zero for fixed-tilt systems, moderate for single-axis systems, and highest for dual-axis systems, consistent with the complexity of their mechanical structures.

The second component is the annual operational expenditure (OPEX). Fixed-tilt systems incur only a constant baseline cost, while tracking systems require additional maintenance due to motorized joints, sensors, gearboxes, and control units. To capture the increasing wear-and-tear of mechanical components over time, we model the tracker-related O&M using an exponential escalation function. When the system is newly installed, the O&M is close to its initial value O_0, but it gradually increases as aging accelerates mechanical stress. This escalation continues until it reaches a saturation ceiling O_{max}, beyond which maintenance effort cannot grow further. Therefore, the annual operational cost in year t is written as:

$$\mathrm{OPEX}(t) = O_{\mathrm{fixed}} + O_{\mathrm{tracker}} = O_{\mathrm{fixed}} + \min\left(O_{\mathrm{max}},\ O_0 e^{k(t-1)}\right)$$

Here, the parameters O_0, k, and O_{max} for each system type are also provided in Figure 1. Static systems experience no aging-driven increase, while single-axis and dual-axis systems exhibit progressively higher O&M burdens due to more frequent mechanical operations and the larger number of moving components.

Having obtained expressions for both CAPEX and OPEX, we compute the Levelized Cost of Energy (LCOE), which discounts the cost and energy flows over the entire

Table 2 Symbols and Explanation

Symbol	Unit	Explanation
P_{rated}	kW	Installed (rated) capacity of the photovoltaic system.
C_{mod}	yuan/kW	Cost of photovoltaic modules per unit installed capacity.
C_{inv}	yuan/kW	Cost of inverters per unit installed capacity.
C_{bos}	yuan/kW	Balance-of-system cost, including wiring, combiner boxes, transformers, etc.
C_{rack}	yuan/kW	Cost of mounting structures or support racks per unit installed capacity.
C_{tracker}	yuan/kW	Additional capital cost of installing a single-axis or dual-axis tracking system.
C_{perm}	/	Cost multiplier accounting for permitting, labor, engineering, land preparation, and construction overhead.
O_{fixed}	yuan/yr	Annual fixed operation and maintenance (O&M) cost, independent of tracking technology.
O_0	yuan/yr	Initial annual O&M cost associated with the tracking system (e.g., inspection, lubricating joints, replacing motors).
k	1/yr	Aging-related O&M escalation rate capturing increased mechanical wear and failure probability in trackers.
$O_{\max}$	yuan/yr	Upper bound on annual tracker-related O&M cost due to saturation of maintenance effort: $O_{\max} = O_0 e^{24 \cdot k}$
O_{tracker}	yuan/yr	Age-dependent additional O&M cost of the tracker: $O_{\text{tracker}}(t) = \min\left(O_{\max}, O_0 e^{k(t-1)}\right)$.
CAPEX	yuan	Total upfront capital expenditure for system installation.
$\text{OPEX}(t)$	yuan/yr	Total annual operational expenditure at year t, including both fixed O&M and tracker-related O&M.
LCOE	yuan/kWh	Levelized Cost of Energy, representing the average cost per unit of electricity generated over the project lifetime.
$E_{\text{year},t}$	kWh	Annual electricity generation in year t.
r	–	Discount rate, used to calculate the present value of future cash flows(normally 0.07).
N	years	Project lifetime, the total number of years over which the system operates.
t	years	Time index, representing a specific year in the project lifetime (ranges from 1 to N).

Figure 1 Data Table

Parameters	Static	Single-axis	Dual-axis
p_rated(kW)	1	1	1
c_mod(yuan/kW)	800	800	800
c_inv(yuan/kW)	800	800	800
c_bos(yuan/kW)	2800	3000	3200
c_rack(yuan/kW)	300	0	0
c_tracker(yuan/kW)	0	1400	3000
c_perm	3%	3%	3%
CAPEX (yuan)	4841	6180	8034
O_fixed(yuan/kW·yr)	120	120	120
O_0(yuan/kW·yr)	0	60	150
k	/	0.05	0.06

project lifetime. Because LCOE represents the long-run average cost of generating one kilowatt-hour of electricity, it provides a direct and objective benchmark for comparing the cost-effectiveness of the three installation configurations. The mathematical form is:

$$LCOE = \frac{CAPEX + \sum_{t=1}^{N} \frac{OPEX_t}{(1+r)^t}}{\sum_{t=1}^{N} \frac{E_{year,t}}{(1+r)^t}}$$

Here $E_{\text{year},t}$ is the annual electricity output in year t, which differs among the three configurations due to differences in solar tracking capability. Because LCOE incorporates both energy gain and cost inflation simultaneously, it naturally reveals whether the additional energy captured by trackers outweighs their higher capital and operational costs.

2.3 Application

We choose three cities to apply this model: Chongqing, Urumqi, and Lhasa. They are chosen for distinguished levels of sunlight, with Lhasa expected to have the most available solar energy and Chongqing the least. We have developed a code to calculate the ultimate electricity output in each city. Input data include geographic data, climatic data, and inverter data. Since all these data are the same for industrial and private installation of photovoltaic panels, we do not discriminate between these two types.

Geographic ones involve the cities' latitude, longitude, and altitude, which determine the AOI and air mass.

Climatic data consist of the surface tilt and azimuth of panels and local sunlight intensity to determine the irradiance of beam and diffusion.

Inverter data encompass the rating voltage of direct and alternating current and the temperature of working photovoltaic cells.

As a result shown by Figure 2, we find that in each city, dual-axis configuration produces significantly more electricity than both of the others, and single-axis panels have slightly greater electricity production than fixed ones. In Urumqi and Lhasa, dual-axis panels generate roughly twice as much electricity as fixed ones do. Furthermore, it turns out that Lhasa's panels produce the greatest amount of electricity and Chongqing's produced the least, which validates the practicality of our model.

Afterward, we apply the economic model described in the last subsection to in-

Figure 2

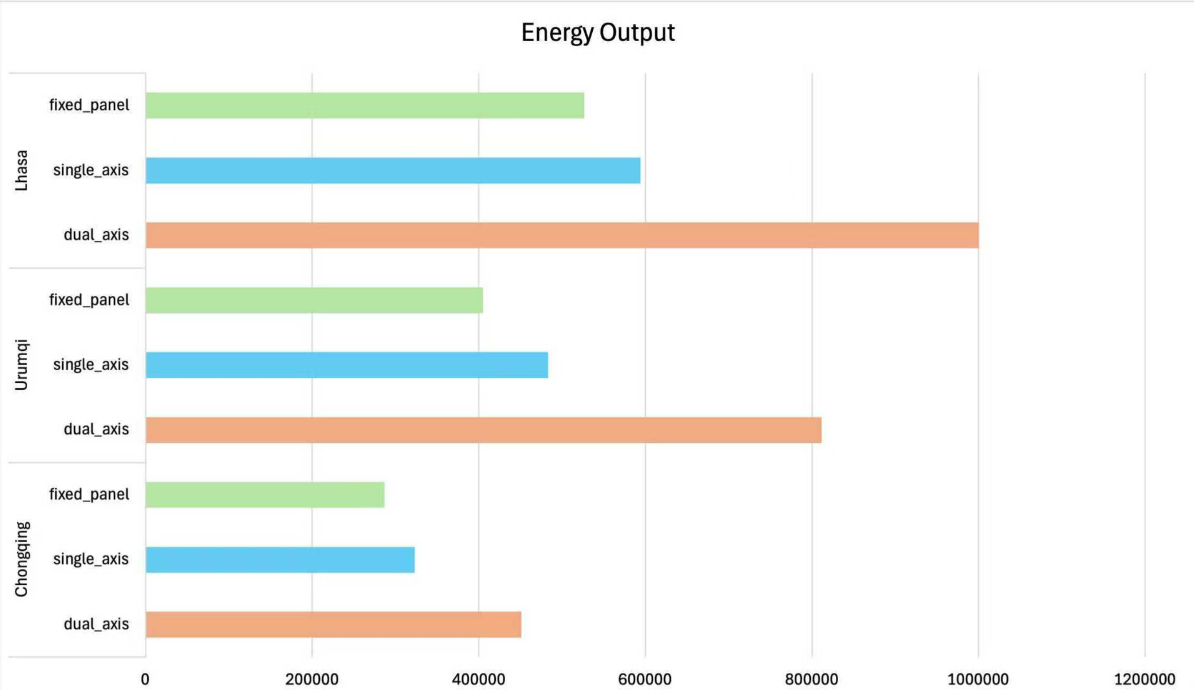

	Chongqing			Urumqi			Lhasa		
	dual_axis	single_axis	fixed_panel	dual_axis	single_axis	fixed_panel	dual_axis	single_axis	fixed_panel
Energy Output	450999.9909	323125.689	286581.6751	811457.3695	483126.2862	405455.5798	1000479.013	594331.03	526916.2164

vestigate whether complex equipment of axes results in excessive expenses that undermine their economic effects. Figure 3 demonstrates the results:

In cities at high altitudes- Lhasa and Urumqi- the profits of a large amount of electricity production by dual-axis panels are not offset by higher costs of installation and maintenance. The cost per kWh of dual-axis configuration for the two cities is

Figure 3 Cost/kWh of Power Production

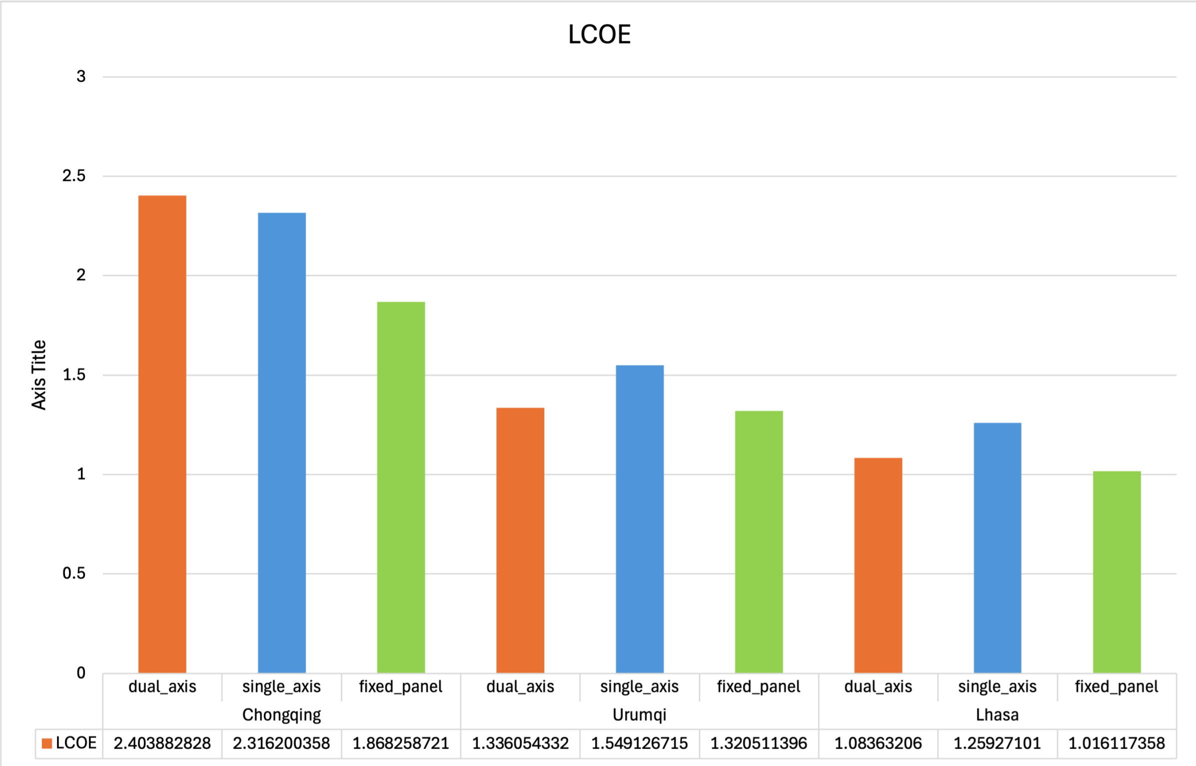

either lowest or grossly the same as that of fixed configuration. It implicates that without increasing much costs, dual-axis panels can still produce prominently more electricity. On the other hand, the cost of single-axis panels is always the highest. This is probably because of the subtly larger amount of electricity produced and higher installation and maintenance costs.

However, in Chongqing, the cost of electricity production is proportional to the complexity of panels. Dual-axis ones are the most costly while fixed ones are the cheapest. It likely results from the fact that Chongqing has low altitude and therefore receives much less intense sunlight, reducing the utility of tracking systems.

3 Problem 2

Considering to extend the model to other countries and areas, since the power-output model has taken geological factors into account, we only need to modify the 'economic-effect' part to guarantee the accuracy of results. To be specific, parameters such as C_{mod}, C_{inv}, and C_{bos} should be adjusted to simulate real situations in the countries we consider about. For example, if we want to extend the model to U.S. using local prices, we record the parameters in Figure 4 as following:

Figure 4 Data Table

Parameters	Static	Single-axis	Dual-axis
P_rated (kW)	1	1	1
c_mod (USD/kW)	400	400	400
c_inv (USD/kW)	150	150	150
c_bos (USD/kW)	550	580	620
c_rack (USD/kW)	200	0	0
c_tracker (USD/kW)	0	700	1,500
c_perm	3%	3%	3%
CAPEX (USD)	1,339	1,885	2,741
O_fixed (USD/kW·yr)	11	11	11
O_0 (USD/kW·yr)	0	10	20
k (1/yr)	/	0.03	0.04

4 Problem 3

Considering a 'manually adjusted mount' that permits changing the panel's position during the regular cleaning of the panel- once every 6 months, we can adjust the function of annual operational cost in year t, rewriting it as:

$$\text{OPEX}(t) = O_{\text{fixed}} + O_{\text{tracker}} = O_{\text{fixed}} + 2 \cdot C_{\text{adj}}$$

in which C_{adj} represents the cost for each adjustment in channels position. '2' represents the times for adjustment per year. Based on the results from previous problems, the dominant factor of economic effects of different installation strategies, in areas with affluent sunlight, is not the fixed cost (installation) or the variable cost of maintenance. By contrast, the most influential factor is the electricity output. Therefore, it is predictable that the adjusted mount would result in less cost per kWh in Chongqing yet little effects in Lhasa and Urumqi.

5 Problem 4

In conclusion, the trackers play a significant role in increasing the efficiency of capturing solar energy, but only in areas with intense sunlight, more complicated installation and maintenance will not offset the economic benefits of the enormous rise in power production. Chongqing, for example, is located at a much lower altitude than Lhasa and Urumqi, thus having the lowest cost per kWh in power production. Dual-axis panels, in particular, can double the electricity production in all considered cases. Traditional fixed photovoltaic panels, on the other hand, do not produce satisfactory results, though characterized by the lowest fixed cost (of installation).

With the urgent need for clean energy, the tracking system has been far more than a ’toy’; instead, by promoting the application of advanced tracking system, both energy crisis and pollution can be mitigated, and it might serve as an answer to sustainable development.

References

[1] IEA PVPS. Trends in Photovoltaic Applications 2024 [R]. Paris: IEA PVPS.https://doi.org/10.69766/JNEW6916

[2] IEA PVPS. Trends in Photovoltaic Applications 2025 [R]. Paris: IEA PVPS.https://doi.org/10.69766/NCNN2417

[3] Kasten F, Young A T. Revised optical air mass tables and approximation formula[J]. Applied optics, 1989, 28(22): 4735-4738.

[4] Kratochvil J A, Boyson W E, King D L. Photovoltaic array performance model[R]. Sandia National Laboratories (SNL), Albuquerque, NM, and Livermore, CA (United States), 2004.

[5] Dobos A P. PVWatts Version 7 Manual (NREL/TP-6A20-83492)[R]. Golden, CO: National Renewable Energy Laboratory, 2022.

[6] KING W, GONZALEZ S, GALBRAITH G M, et al. Performance model for grid-connected photovoltaic inverters [R]. Albuquerque: Sandia National Laboratories, 2004. (SAND2004-9695).